Engineering Science and Technology, an International Journal 19 (2016) 518–530

HOSTED BY

ELSEVIER

Contents lists available at ScienceDirect

Engineering Science and Technology, an International Journal

journal homepage: http://www.elsevier.com/locate/jestch

Full Length Article

Indirect fractional order pole assignment based adaptive control

Samir Ladaci [a,b,*], Yassine Bensafia [c]

[a] National Polytechnic School of Constantine, E.E.A. Department, Ali Mendjli, Constantine 25000, Algeria
[b] SP-Lab Laboratory, Department of Electronics, University of Constantine 1, Route de Ain El-Bey, Constantine 25000, Algeria
[c] Department of Electrical Engineering, Skikda University, Skikda 21000, Algeria

ARTICLE INFO

Article history:
Received 19 July 2015
Received in revised form
22 August 2015
Accepted 4 September 2015
Available online 21 October 2015

Keywords:
Fractional order control
Fractional adaptive control
Indirect pole placement
Fractional order system

ABSTRACT

The design method of polynomial control laws by mean of pole placement are actually smart solutions to many industrial applications. This category of controllers is very popular in the industry; however most of their applications concern only problems with constant reference signals. In this paper, we propose an indirect adaptive controller by fractional order pole placement. The proposed control strategy is based on the self-tuning control structure and on-line estimation of the plant model parameters using the Recursive Least Squares (RLS) algorithm. To show the effectiveness of the proposed control scheme two simulation examples are presented. The first example is the control of a DC motor angular speed and the second one is the control of an air-lubricated capstan drive for precision positioning. Improvement in the system control dynamical behavior compared to classical control scheme has been shown for the two illustrative examples.

1. Introduction

Fractional adaptive control is a rapidly growing research topic [1]. Since the pioneering works of Vinagre et al. [2] and Ladaci and Charef [3] a decade ago, a great number of fractional adaptive control approaches have been developed. Some researchers have been interested in the Fractional Order Model Reference Adaptive Control (FOMRAC) [4–8]; others have investigated the fractional adaptive PID control domain [9,10]. Fractional order adaptive High-Gain control [11,12], fractional IMC-based adaptive control [13] and robust fractional order adaptive control [14,15] have also been introduced. Very recently fractional adaptive extremum seeking control has been investigated in Neçaibia et al. [16]. Because of the fractional, integral and derivative orders, the fractional order adaptive control laws offer new maneuver margins to the design engineers for control parameters tuning making it possible to improve significantly the controlled system's behavior and robustness. Applications of fractional order control are as various as robotics [3,9,14], autonomous guided vehicle (AGV) [17], hydraulic flight simulator [18], automatic voltage regulator [6], position servo systems [19], and renewable energy systems [20–22].

In this paper we propose a new fractional order adaptive control strategy based on the on-line indirect pole placement approach, by imposing fractional order poles while identifying the process model parameters in real time by mean of the least square estimation (LSE) method. The resulting fractional order control dynamics are implemented by making use of the so-called singularity function approximation method [23]. The rational function approximation obtained translates efficiently the controller synthesis to the classical integer order algebraic domain allowing easy computing of the control law from the general Diophantine equation. Two simulation examples are given to illustrate the enhanced performance obtained by the proposed indirect adaptive fractional pole placement control scheme and the usefulness of this real time control algorithm. The first example presents the application of this technique to the velocity control of a DC motor while as the second concerns the control of an air-lubricated capstan drive for precision positioning.

This paper is organized as follows: Section 2 presents some mathematical basics of the fractional calculus and the considered approximation approach for fractional order functions. Section 3 introduces the proposed indirect fractional order adaptive pole placement algorithm with the estimation method. Illustrative examples of control applications are presented in Section 4 to show the good performance of this control technique; finally some concluding remarks in Section 5 comment on this work.

2. Fractional order systems

The 19th century offered the major developments of the fractional-order derivative concept. Some recent reference books [24,25] provide a good source for the fractional calculus state of the art. However, application of fractional-order operators in dynamic feedback control systems is just a recent topic but it is gathering growing interest [26–29].

* Corresponding author. Tel.: +213 777809846; fax: +213 31785174.
E-mail address: samir_ladaci@yahoo.fr (S. Ladaci).
Peer review under responsibility of Karabuk University.

http://dx.doi.org/10.1016/j.jestch.2015.09.004

2.1. Basic definitions

Fractional order integrals and derivatives are generalizations of the classical (integer order) ones. Non-integer order fundamental operators are commonly represented as ${}_aD_t^{\mu}$ where a and t are the limits and $\mu(\mu \in \Re)$ the order of the operation. Researches in such an ambiguous topic leaded mathematicians to many (different) definitions of this operator [25].

One of the fractional integro-differential operator definitions that have most popularity is the Riemann–Liouville (RL) definition:

$$ {}_aD_t^{\mu} f(t) = \frac{1}{\Gamma(1-\mu)} \frac{d^n}{dt^n} \int_a^t (t-\xi)^{-\mu} f(\xi) d(\xi) \quad (1) $$

where $\Gamma(.)$ is the Euler's Gamma function, $(a,t) \in \mathbb{R}^2$ with $a < t$ and n an integer.

The Laplace transform of the Riemann–Liouville fractional operator (1) under null initial conditions for the order μ, $(0 < \mu < 1)$ is given by

$$ L\{{}_aD_t^{\pm\mu} f(t); s\} = s^{\pm\mu} F(s) \quad (2) $$

A single input single output (SISO) fractional order system can be represented by the following transfer function,

$$ F(s) = \frac{b_m s^{\beta_m} + b_{m-1} s^{\beta_{m-1}} + \ldots + b_0 s^{\beta_0}}{a_n s^{\alpha_n} + a_{n-1} s^{\alpha_{n-1}} + \ldots + a_0 s^{\alpha_0}} \quad (3) $$

where α_i and β_j are real numbers such that,

$$ \begin{cases} 0 \le \alpha_0 < \alpha_1 < \ldots < \alpha_n \\ 0 \le \beta_0 < \beta_1 < \ldots < \beta_m \end{cases} $$

and s is Laplace operator.

2.2. Approximated fractional second-order transfer function

The main problem with fractional order control design is that the resulting functions are of infinite dimension, whereas the implementation of such controllers needs to be realized by finite dimensional approximated linear filters.

This implies for the present work the need of an approximation method in order to replace the resulting fractional order functions by quasi-equivalent rational transfer functions in order to assign fractional order dynamics to the controlled system closed loop. In order to achieve this goal, we shall use the simple but popular *singularity function method* for approximation in the frequency domain [23,30].

For the need of the case study below, let us focus on the fractional standard second-order transfer function given by:

$$ G_f(s) = \frac{1}{\left(\frac{s^2}{\omega_n^2} + 2\xi \frac{s}{\omega_n} + 1\right)^{\beta}} \quad (4) $$

where ξ is the damping factor, ω_n the proper pulse and $0 < \beta < 1$.

This function is usually employed as reference model in control systems design because of the well known properties of the system (4) in terms of the fractional order β and the damping factor effects on time response [31].

The singularity function method makes it possible to approximate the fractional order transfer function (4) by a quotient of polynomials in s. Two cases are distinguished

- **Case** $0 < \beta < 0.5$:

We can express the function (4) as follows:

$$ G_e(s) = \frac{\left(\frac{s}{\omega_n} + 1\right)\left(\frac{s}{\omega_n + 1}\right)^{\eta}}{\left(\frac{s^2}{\omega_n^2} + 2\alpha \frac{s}{\omega_n} + 1\right)} \quad (5) $$

with $\alpha = \xi^{\beta}$ and $\eta = 1 - 2\beta$, which can also be approximated by the function,

$$ G_e(s) \approx \frac{\left(\frac{s}{\omega_n} + 1\right)}{\left(\frac{s^2}{\omega_n^2} + 2\alpha \frac{s}{\omega_n} + 1\right)} \frac{\prod_{i=1}^{N-1}\left(1 + \frac{s}{z_i}\right)}{\prod_{i=1}^{N}\left(1 + \frac{s}{p_i}\right)} \quad (6) $$

The singularities (poles p_i and zeros z_i) are given by the following formulas:

$$ p_i = (ab)^{i-1} a z_1 \quad i = 1, 2, 3, \ldots, \quad (7) $$

$$ z_i = (ab)^{i-1} z_1 \quad i = 2, 3, \ldots, N-1 \quad (8) $$

with,

$$ z_1 = \omega_n \sqrt{b} \quad (9a) $$

$$ a = 10^{\frac{\varepsilon_p}{10(1-\eta)}} \quad (9b) $$

$$ b = 10^{\frac{\varepsilon_p}{10\eta}} \quad (9c) $$

$$ \eta = \frac{\log(a)}{\log(ab)} \quad (9d) $$

ε_p is the tolerated error in dB. The approximation order N is calculated by fixing the working frequency bandwidth, specified by ω_{max} such that: $p_{N-1} < \omega_{max} < p_N$, which leads to the following value:

$$ N = \text{Integer part of} \left[\frac{\log\left(\frac{\omega_{max}}{p_1}\right)}{\log(ab)} + 1 \right] + 1 \quad (10) $$

$G_e(s)$ can then be rewritten under the form of a parametric function of order $N+2$ as in Equation (11).

$$ G_e(s) = \frac{b_{m_0} s^N + b_{m_1} s^{N-1} + \ldots + b_{m_N}}{s^{N+2} + a_{m_1} s^{N+1} + \ldots + a_{m_{N+2}}} \quad (11) $$

The coefficients a_{m_i} and b_{m_i} are computed from the singularities p_i, z_i as well as α and ω_n.

- **Case** $0.5 < \beta < 1$:

The fractional transfer function is rearranged as follows:

$$ G_e(s) = \frac{\left(\frac{s}{\omega_n} + 1\right)}{\left(\frac{s^2}{\omega_n^2} + 2\alpha \frac{s}{\omega_n} + 1\right)\left(\frac{s}{\omega_n + 1}\right)^{\eta}} \quad (12) $$

where $\alpha = \xi^{\beta}$ and $\eta = 2\beta - 1$, developed as mentioned above with the following values of poles and zeros:

$$ p_i = (ab)^{i-1} p_1 \quad i = 1, 2, 3, \ldots, N \quad (13) $$

$$ z_i = (ab)^{i-1} a p_1 \quad i = 2, 3, \ldots, N-1 \quad (14) $$

$$p_1 = \omega_n \sqrt{b} \tag{15a}$$

$$a = 10^{\frac{\varepsilon_p}{10(1-\eta)}} \tag{15b}$$

$$b = 10^{\frac{\varepsilon_p}{10\eta}} \tag{15c}$$

$$\eta = \frac{\log(a)}{\log(ab)} \tag{15d}$$

$G_e(s)$ can than be written under the form of Equation (11).

3. Indirect fractional adaptive control strategy

The self-tuning regulator (STR) makes it possible to charge numerical processors with many complex control tasks in real time such as modeling, control law design, implementation, and validation. The adaptive auto-tuning control design presents particular specifications: the considered design techniques have to be adaptable to real time computation making the controller parameters available at every sampling period. This means that basic automatic engineering methods (such as frequency methods, root locus, etc.) are not useful here.

Starting from the assumption that the process model structure is known (or specified), the plant model parameters are estimated online, and the block labeled 'Estimation' in Fig. 1 gives an estimate that will be used to compute the polynomial controller coefficients. This scheme involves also some numerical calculus that is necessary to perform a design of a controller with a particular method and a number of design parameters that can be chosen externally [32].

The design problem is called the underlying design problem for systems with known parameters. The block labeled 'Controller' is a realization of the regulator whose parameters result from the control design.

3.1. Pole/zero placement

The pole/zero placement approach is based on a very simple reasoning. The desired dynamics of the closed loop control system are specified by means of the singular values of a transfer function that is equated with the closed-loop transfer function of the real process model. The controller parameters are unknown in this scheme but they are closely related with the process parameters.

Consider the case of a well known causal system transfer function represented by:

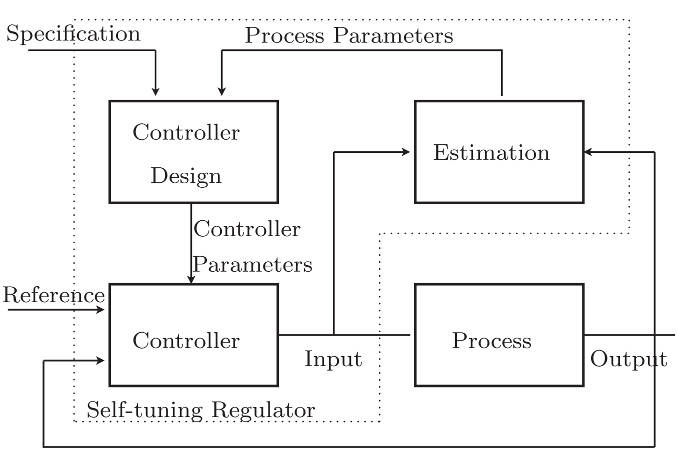

Fig. 1. Self-tuning regulator.

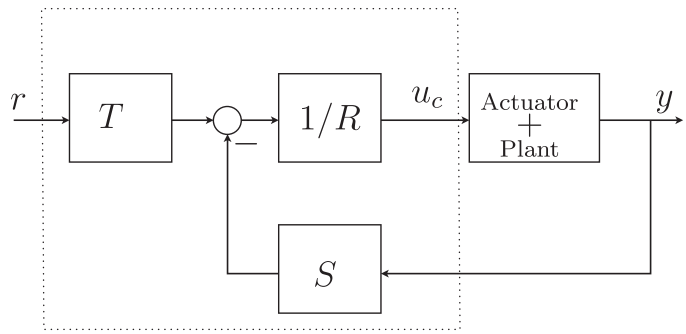

Fig. 2. Two parameter controller topology.

$$G_p(q) = \frac{B(q)}{A(q)} \tag{16}$$

where q is the shift operator defined by: $qf(k) = f(k+1)$ and $deg(A) > deg(B)$, and A and B are coprime polynomials. One has to calculate the controller parameters in order to obtain the desired dynamics of the closed-loop system given by the model expressed by the discrete-time transfer function:

$$G_m(q) = \frac{B_m(q)}{A_m(q)} \tag{17}$$

The control structure capable to solve this problem is given in Fig. 2.

It is well known that the general linear regulator can be given by the formula:

$$Ru(t) = Tu_r(t) - Sy(t) \tag{18}$$

where R, S and T are polynomials, u is the control signal, y the process output and u_r the reference signal. This control law represents a negative feedback with the transfer operator $-\frac{S}{R}$ and a direct feedforward action with the transfer operator $\frac{T}{R}$.

By eliminating u in Equation (18) we obtain the following closed loop equations,

$$\begin{aligned} y(t) &= \frac{BT}{AR+BS}u_r(t) + \frac{BR}{AR+BS}v(t) \\ u(t) &= \frac{AT}{AR+BS}u_r(t) + \frac{BS}{AR+BS}v(t) \end{aligned} \tag{19}$$

where v is a disturbance. The characteristic polynomial of the closed loop system is then,

$$AR + BS = A_r \tag{20}$$

The key idea of this design method is to specify the desired closed-loop characteristic polynomial, A_r. Whereas, polynomials R and S can be determined from Equation (20).

In this procedure, the main design parameter is the polynomial A_r, that is chosen to impose some desired properties and dynamic behavior to the closed loop system. Equation (20) called the *Diophantine Equation* and also the *Bezout Identity* plays an important role in control theory algebra. Factor the B polynomial as

$$B = B^+B^- \tag{21}$$

where B^+ is a monic polynomial whose zeros are stable and so well damped that they can be canceled by the controller and B^-

corresponds to unstable factors that cannot be canceled. A compatibility condition is that B^- must also be a factor of B_m. Hence

$$B_m = B^- B'_m \tag{22}$$

The closed-loop characteristic polynomial thus has the form

$$A_r = A_o A_m B^+ \tag{23}$$

where A_o is called the observer polynomial, to be designed such that Equation (20) have a solution.

Since B^+ is a factor of B and A_r, it follows that,

$$R = R' B^+ \tag{24}$$

The following causality condition has to be verified:

$$deg\ A_m - deg\ B_m \geq deg\ A - deg\ B = d_0 \tag{25}$$

The chosen regulator has to be of the minimum possible degree, and should not introduce further delays in the control loop. This implies that polynomials R, S and T must have the same degree.

The following algorithm usually known as "minimal degree pole placement" reports the main steps for the considered control law design procedure:

Algorithm 1. Minimal degree pole placement

- **Data:** *Polynomials A, B*
- **Specifications:** *Polynomials A_m, B_m and A_o*
- **Step 1:** *factorize B such that $B = B^+B^-$, where B^+ is monic*
- **Step 2:** *find a solution R' and S with deg $S <$ deg A from*

$$AR' + B^- S = A_o A_m \tag{26}$$

- **Step 3:** *from $R = R'B^+$ and $T = A_o B'_m$, compute the control signal from the Diophantine Equation (18).*

3.2. Estimation

Many recursive estimation methods may be used to estimate the coefficients of the polynomials A and B. In this work we will use the simple but efficient Recursive Least-Squares (RLS) estimator.

Let the process model be written as follows (we neglect noises for simplification sake),

$$y(t) = -a_1 y(t-1) - a_2 y(t-2) - \ldots - a_n y(t-n) + b_0 u(t-d_0) + \ldots + b_m u(t-d_0-m) \tag{27}$$

One can notice this system linearity for the parameters with the degree $max(n, d_0 + m)$. Rewriting it as follows,

$$y(t) = \varphi^T(t-1)\theta \tag{28}$$

where

$$\theta^T = (a_1\ a_2 \ldots a_n\ b_0 \ldots b_m)$$

$$\varphi^T(t-1) = (-y(t-1) \ldots -y(t-n)\ u(t-d_0) \ldots u(t-d_0-m))$$

The recursive least-squares estimator with exponential forgetting is given by:

$$\begin{aligned}
\breve{\theta}(t) &= \breve{\theta}(t-1) + K(t)\varepsilon(t) \\
\varepsilon(t) &= y(t) - \varphi^T(t-1)\breve{\theta}(t-1) \\
K(t) &= P(t-1)\varphi(t-1) \times \left(\lambda + \varphi^T(t-1)P(t-1)\varphi(t-1)\right)^{-1} \\
P(t) &= I - K(t)\varphi(t-1)P(t-1)/\lambda
\end{aligned} \tag{29}$$

where the parameter λ, called the forgetting factor or discounting factor, is chosen such that $0 < \lambda \leq 1$.

The convergence of the estimates to their true values is conditioned by a good choice of the model structure which needs to be adequate with the controlled plant and the input signals that have to be exciting enough. In the deterministic case, a minimum of $n + m + 1 + max(n, m + d_0)$ sampling periods is necessary for the algorithm to converge [32].

3.3. Fractional order pole assignment

The principle control design objective is to impose a fractional order characteristic polynomial A_m^f in the Algorithm 1 and precisely in the Diophantine Equation (26).

Let us consider the desired reference model (desired dynamic poles) G_m to be of the fractional order standard form (4). By using the singularity function approximation method we compute its approximated transfer function $G_m^f = \frac{B_m^f}{A_m^f}$ as given in Equation (11).

As the degree of G_m^f is higher than that of A, it is straightforward to take the observation polynomial $A_o = 1$. Thus: $A_r^f = A_m^f$. The Diophantine Equation (26) becomes then,

$$AR' + B^- S = A_m^f \tag{30}$$

where A_m^f is the denominator of the approximating function. By combining the RLS estimation of Equation (30) with the minimal degree pole placement method for control design given by the Algorithm 1, we obtain the following fractional order self-tuning regulator:

Algorithm 2. Indirect fractional self-tuning regulator

- **Specifications:** *Parameters ω_n, ξ, order β of the model (4). Compute the approximation $\frac{B_m^f}{A_m^f}$ as given in Equation (30).*
- **Step 1:** *Estimate the coefficients of polynomials A and B in Equation (27) using the RLS method given by Equation (30).*
- **Step 2:** *Apply the minimal degree pole placement technique given by algorithm 1 where polynomials A and B are the estimations obtained in* **step 1**. *Polynomials R, S and T of the control law are computed.*
- **Step 3:** *Calculate the command variable from Equation (30).*

Repeat **steps 1, 2 and 3** *at every sampling period.*

4. Simulation results

In this section we will apply the proposed fractional order adaptive control strategy to the control of two industrial plants and compare their performance with that obtained for the classical integer order adaptive pole placement controller. Firstly we will apply the proposed control strategy to a Direct Current Motor velocity [33], which a simple and widely used process in industrial applications. A second application is the control of air-lubricated capstan drive for precision positioning [34] which is a more complex system involving also a DC motor actuator.

4.1. DC motor angular velocity control

4.1.1. Plant modelization

A great number of industrial applications make use of the DC motor as actuator particularly for low power processes. The motor provides rotary motion directly and, if coupled with wheels or drums and cables, it can provide translational motion. Fig. 3 shows the electric equivalent circuit of the armature and the free-body diagram of the rotor.

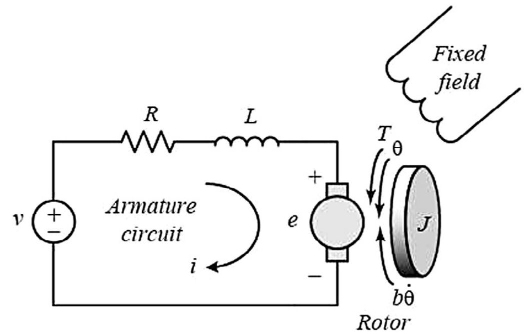

Fig. 3. The structure of a DC motor.

For the present simulation study, the voltage source (V) applied to the motor's armature is assumed to be the system's input, while the output is the rotational speed of the shaft $d(\theta)/dt$. The rotor and shaft are assumed to be rigid. We further assume a viscous friction model, that is, the friction torque is proportional to shaft angular velocity. Table 1 presents the main physical parameters for the system.

From the scheme of Fig. 3, we can derive the following governing equations based on Newton's 2nd law and Kirchhoff's voltage law.

$$\begin{cases} J\ddot{\theta} + b\dot{\theta} = ki \\ L\dfrac{di}{dt} + Ri = V - k\dot{\theta} \end{cases} \tag{31}$$

In frequency Laplace domain, we obtain the following open-loop transfer function relating the output $\dot{\theta}(s)$ to the input $V(s)$, after some algebraic manipulations.

$$\frac{\dot{\theta}(s)}{V(s)} = \frac{k}{(Js+b)(Ls+R)+k^2} \tag{32}$$

The numerical values of the parameters from Table 1 give:

$$\frac{Y}{U} = \frac{81018}{s^2 + 260.7s + 2394} \tag{33}$$

4.1.2. Integer order adaptive pole placement control

Taking a sampling period $T = 0.04\ s$, the system (33) is reformulated in the discrete time domain as,

$$G(q) = \frac{9.816q + 0.9112}{q^2 - 0.683q + 2.959\,10^{-005}} \tag{34}$$

The desired poles to be imposed to the process are those of the standard second order transfer function (4) with $\beta = 1$ (integer case), $\omega_n = 10$ and $\xi = 0.95$.

We use the RLS algorithm (30) to estimate the process model parameters, and after simplification of the Bezout identity (20), we obtain the control law,

Table 1
The DC Motor physical parameters.

Specification parameter	Value
Moment of inertia of the rotor (J)	0.018 kg.m^2
Motor viscous friction constant (b)	0.0055 N.m.s
Electromotive force constant (Ke)	1 V/rad/sec
Motor torque constant (Kt)	0.01 N.m/Amp
Electric resistance (R)	6.25 Ohm
Electric inductance (L)	0.024 H

$$u(k+1) = -r_1 u(k) + t_0 u_r(k+1) - s_0 y(k+1) - s_1 y(k) \tag{35}$$

where u is the control signal, u_r the reference and y the process output.

For the initial values:

$$\theta^T = [-1.5317\ 0.6132\ 1.5325\ 1.2259],\ \lambda = 0.75,$$

we obtain the simulation results of Figs. 4 and 5 for the ideal case and in the presence of 5% magnitude additive output noises, respectively.

The examination of the process output response to a step reference signal show a satisfactory behavior in absence of disturbances and noises: an acceptable response time and a limited overshoot. The simulation results show that the process output y follows the reference signal, with still an acceptable performance even in presence of noises.

4.1.3. Fractional order adaptive pole placement control

The desired fractional order reference model (desired poles) is given by Equation (4) with the parameters: $w_n = 10$, $\xi = 0.95$, $\beta = 0.4$. (The fractional order $\beta = 0.4$ is chosen arbitrarily in a first time for the sake of comparison with the integer order dynamics, then it will be optimized later using a quadratic error criteria).

The resulting discrete time model with the sampling period $T = 0.04\ s$ is given by:

$$G_f(q) = \frac{\begin{array}{c}0.0469q^4 + 0.03919q^3 - 0.004319q^2 \\ -2.292\,10^{-8}q - 5.346\,10^{-25}\end{array}}{\begin{array}{c}q^5 - 1.629q^4 + 0.837q^3 - 0.1289q^2 \\ -3.159\,10^{-19}q + 8.014\,10^{-35}\end{array}} \tag{36}$$

where the characteristic polynomial A_r is the denominator. After resolving the Diophantine Equation (20), we find the control law:

$$\begin{aligned} u(k+1) = &-r_1 u(k) - r_2 u(k-1) - r_3 u(k-2) - r_4 u(k-3) + t_0 u_r(k-2) \\ &- s_0 y(k-2) - s_1 y(k-3) \end{aligned} \tag{37}$$

with $t_0 = 0.0928$.

Taking the initial parameter values:

$$\theta^T = [-1.5317\ 0.6132\ 1.5325\ 1.2259],\ \lambda = 0.75$$

(the same initial values in the integer order case), the simulation results are presented in Figs. 6 and 7 for the ideal case and in presence of 5% magnitude additive output noises, respectively.

One can notice the perfect desired reference velocity following by the process output with an improved performance (fractional order dynamics). Particularly, the overshoot is reduced comparatively to the integer order case and the noises effect is acceptable as expected previously knowing the good robustification properties of fractional order filters [35].

In order to get a better observation of the differences between the fractional case and the integer order case in the noisy experiments, let us define a numerical index I_β as the quadratic error criteria versus the fractional power β of the model reference transfer function given in Equation (4),

$$I_\beta = \sum_{k=N_0}^{N_f} \left(y(kT) - u_r(kT)\right)^2 \tag{38}$$

computed on the time interval $[N_0 T\ N_f T]$.

The resulting values of the index I_β for both the integer and the fractional adaptive pole placement control schemes of the DC Motor in presence and in absence of additive noises are given in Table 2 (The amplitude of random noise being the same in both cases). It

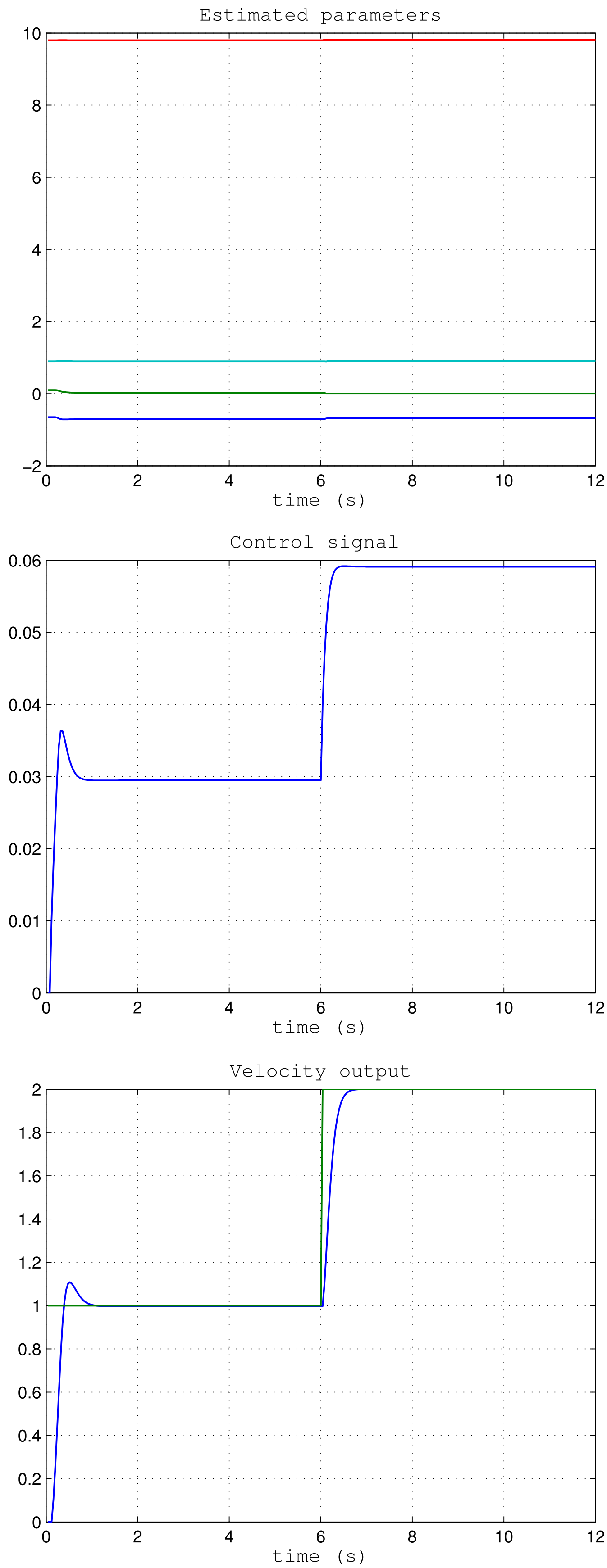

Fig. 4. Integer order adaptive pole placement control of a DC Motor (Ideal case).

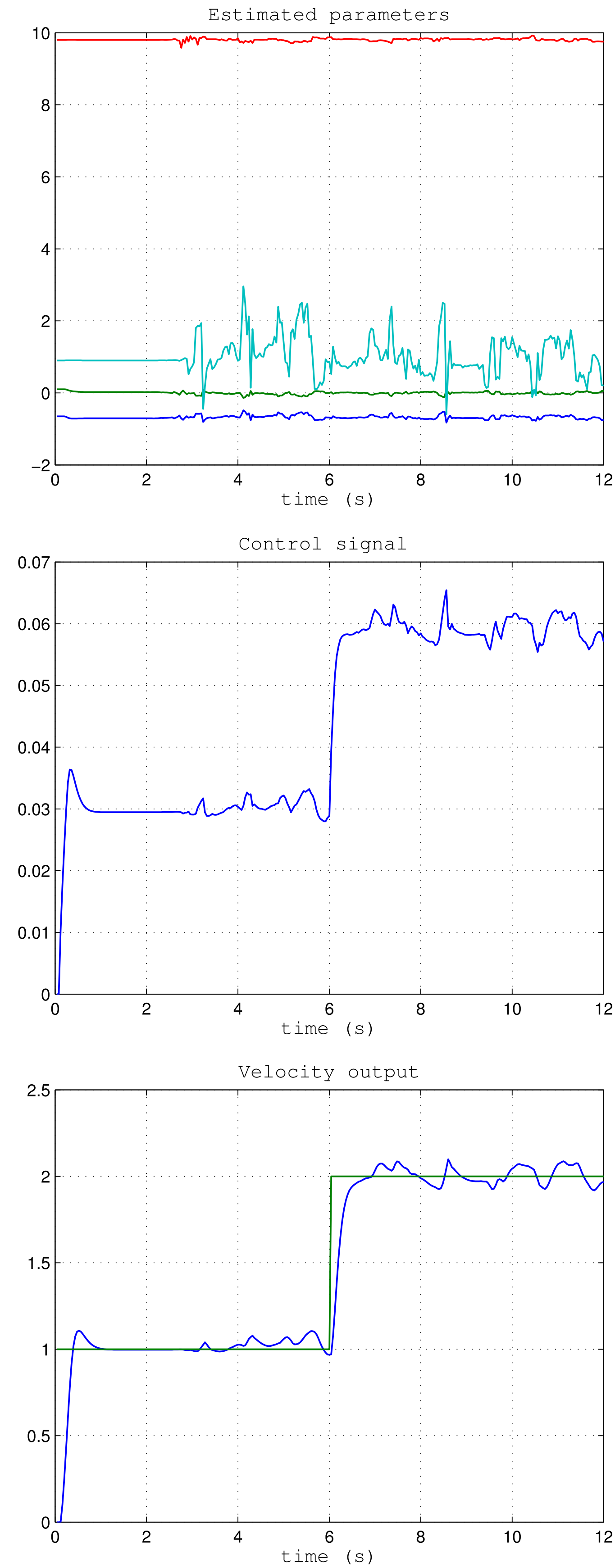

Fig. 5. Integer order adaptive pole placement control of a DC Motor (with output additive noises).

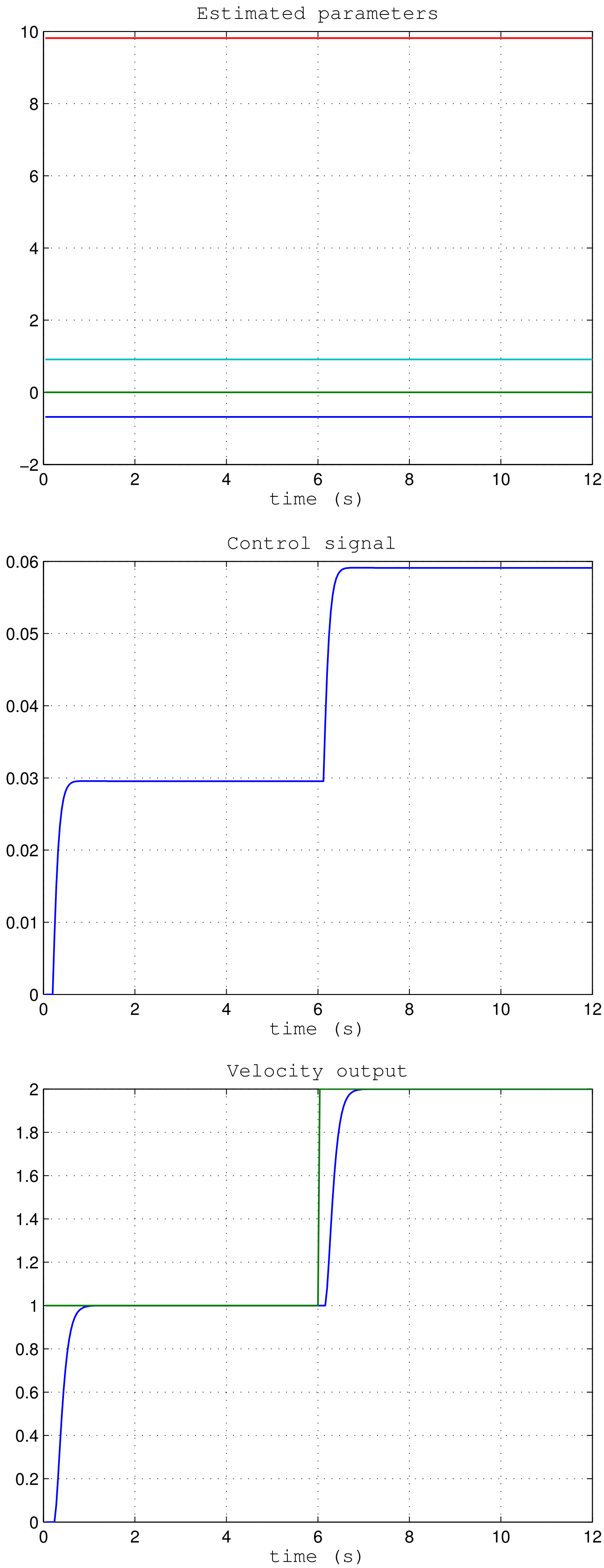

Fig. 6. Fractional order adaptive pole placement control of a DC Motor for $\beta = 0.4$ (Ideal case).

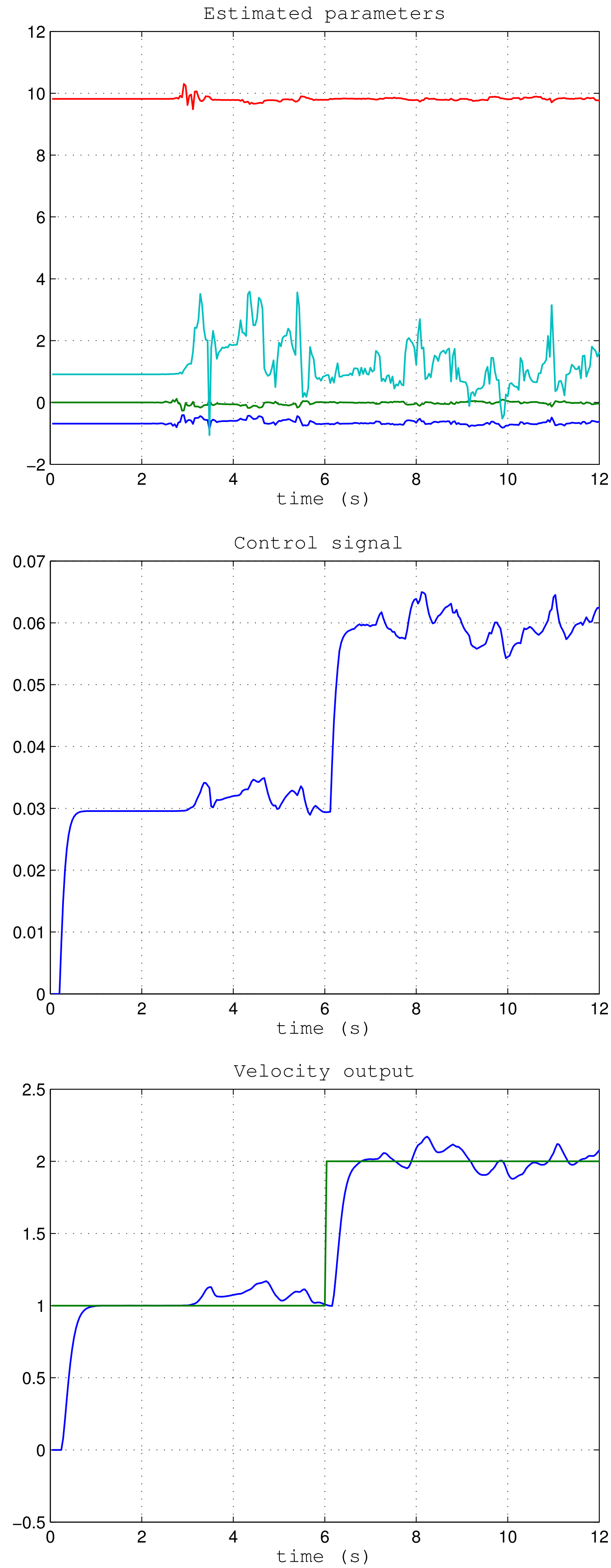

Fig. 7. Fractional order adaptive pole placement control of a DC Motor for $\beta = 0.4$ (with additive noises).

Table 2
Quadratic error criteria VS DC Motor fractional control order.

β	I_β Without perturbation	I_β With additive output perturbation
0.3	2.00	2.42
0.4	2.25	3.02
0.45	2.00	2.31
0.7	2.00	2.34
0.8	**2.00**	**2.23**
0.9	2.00	2.39
1	**1.80**	**3.75**

The use of bold points out results obtained for the integer order (1) vs. the best fractional order.

is obvious from these comparative results that the best disturbance rejection is obtained for the fractional order $\beta = 0.8$ with an improvement rate of about 60% comparatively to the integer order case ($\beta = 1$), even if this latter has sometimes a lower error index in the ideal case (This is due to the dynamics introduced by this higher order approximation filter). Fig. 8 presents the best system behavior obtained for the fractional order $\beta = 0.8$ in the presence of 5% magnitude additive output noises.

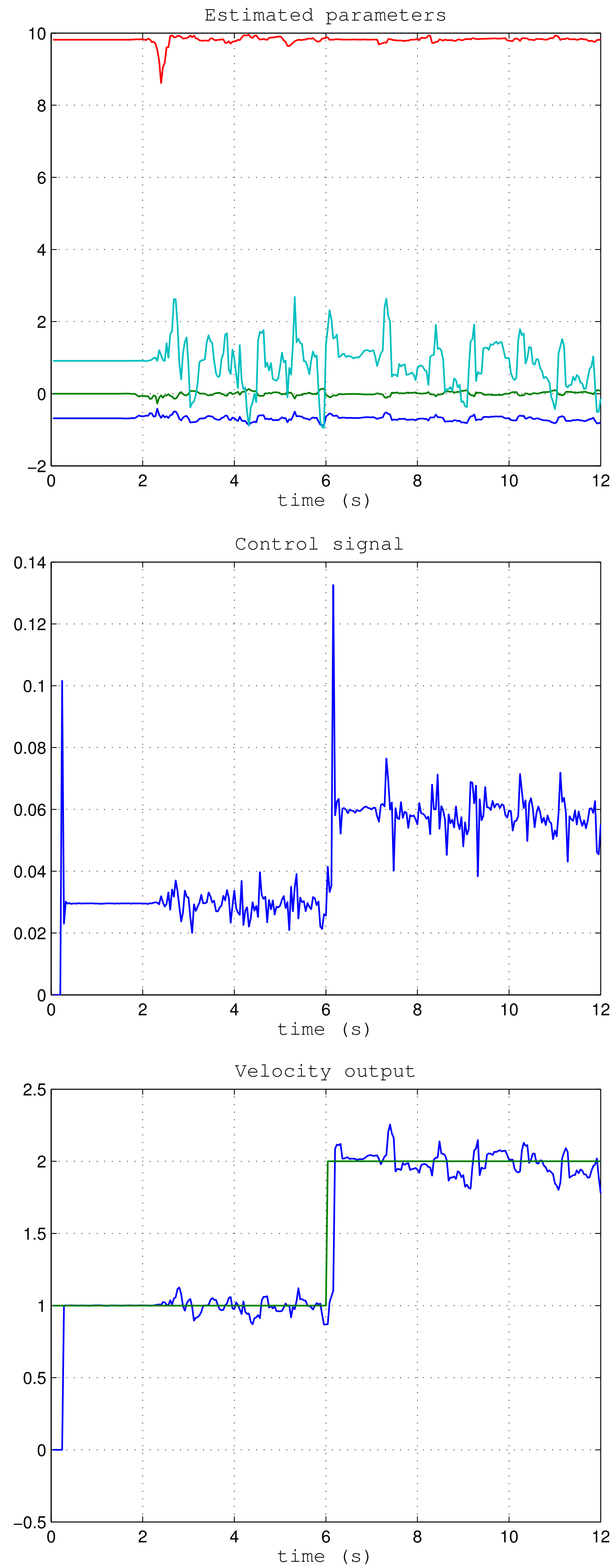

Fig. 8. Fractional order adaptive pole placement control of a DC Motor for $\beta = 0.8$: Best result.

4.2. Air-lubricated capstan drive control

In a positioning system, accuracy and repeatability are the principle necessities, implying robust and disturbance resistant controller.

4.2.1. Plant modelization

Consider the air-lubricated capstan drive represented in Fig. 9. The system identification experiment is described in Chao and Neou [34] and combines the air-lubricated capstan drive, DC servo motor, and air slide. The controller implemented on PC includes a zero-order-hold element accounting for 1 *kHz* sampling period.

The empirical identified plant model is given in the Laplace domain by the transfer function,

$$G_p(s) = \frac{y(s)}{u(s)} = \frac{c}{s^2 + as + b} \tag{39}$$

where u is the control signal, y is the measured (actual) output, a, b and c are the process parameters. The system identification [34] revealed that poles for macro and micro-motion are located very closely together at $-39.1801 \pm j90.4051$ rad/sec and $-41.2584 \pm j94.1516$ rad/sec, with a minor change in system gain (from 0.036 dB to 0.031 dB). The same research work showed that a MRAC scheme was able to control the system in both micro and macro-modes of motion.

Let us consider the macro-motion behavior with the identified model parameters: $a = 78.36$, $b = 9708$ and $c = 9748$.

4.2.2. Integer order adaptive pole placement control

Taking a sampling period $T = 0.001$ *s*, the system (39) is reformulated in the discrete time domain as,

$$G_p(q) = \frac{0.004745(q + 0.9743)}{q^2 - 1.915q + 0.9246} \tag{40}$$

The desired poles to be imposed to the process are those of the standard second order transfer function (4) with $\beta = 1$ (integer case), $\omega_n = 100$ and $\xi = 0.7$.

We use the RLS algorithm (30) to estimate the process model parameters, and after simplification of the Bezout identity (20), we obtain the control law (35),

$$u(k+1) = -r_1 u(k) + t_0 u_r(k+1) - s_0 y(k+1) - s_1 y(k)$$

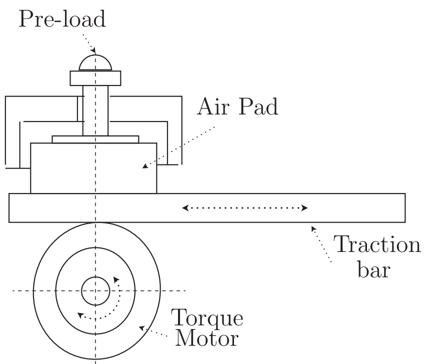

Fig. 9. Air-lubricated capstan drive.

For the initial values:

$\theta^T = [-2.0422\ 0.9496\ 0.0197\ 0.0197], \lambda = 0.9,$

we obtain the simulation results of Figs. 10 and 11 for the ideal case and in the presence of 5% magnitude additive output noises, respectively.

The examination of the process output response to a step reference signal show a satisfactory behavior in absence of disturbances and noises: an acceptable response time and a limited overshoot. The simulation results show that the process output y follows the reference signal, with still an acceptable performance even in presence of noises.

4.2.3. Fractional order adaptive pole placement control

We set the desired fractional order reference model (desired poles) given by Equation (4) with the parameters: $w_n = 100$, $\xi = 0.7$, and $\beta = 0.45$. The resulting discrete time model with the sampling period $T = 0.001$ s is given by:

$$G_f(q) = \frac{0.1208q^3 - 0.1369q^2 + 0.02499q + 2.72\,10^{-6}}{q^4 - 1.869q^3 + 0.9064q^2 - 0.02897q + 5.318\,10^{-19}} \quad (41)$$

where the characteristic polynomial A_r is fourth order denominator polynomial. After resolving the Diophantine Equation (20), we find the control law:

$$u(k+1) = -r_1u(k) - r_2u(k-1) - r_3u(k-2) + t_0u_r(k) - s_0y(k-2) - s_1y(k-3) \quad (42)$$

with $t_0 = 0.9161$.

Taking the initial parameter values:

$\theta^T = [-2.0422\ 0.9496\ 0.0197\ 0.0197], \lambda = 0.9$

(the same initial values in the integer order case), the simulation results are presented in Figs. 12 and 13 for the ideal case and in presence of 10% magnitude additive input noises, respectively.

Figs. 10 and 12 illustrate the satisfactory control results with the proposed adaptive control scheme for respectively the integer order ($\beta = 1$) and the fractional order ($\beta = 0.45$) cases. The performance indexes such as rise time, maximum overshoot, and steady state error are of good level, with a certain improvement in the fractional order controller response regarding the overshoot (almost null) and the control signal shape (less oscillations).

The results of Figs. 11 and 13 which can be considered as disturbance resistance tests, show the very swift recovery of the target position by the on line controlled system when disturbance of 10% command signals intensity was applied on the process in both integer and fractional order cases.

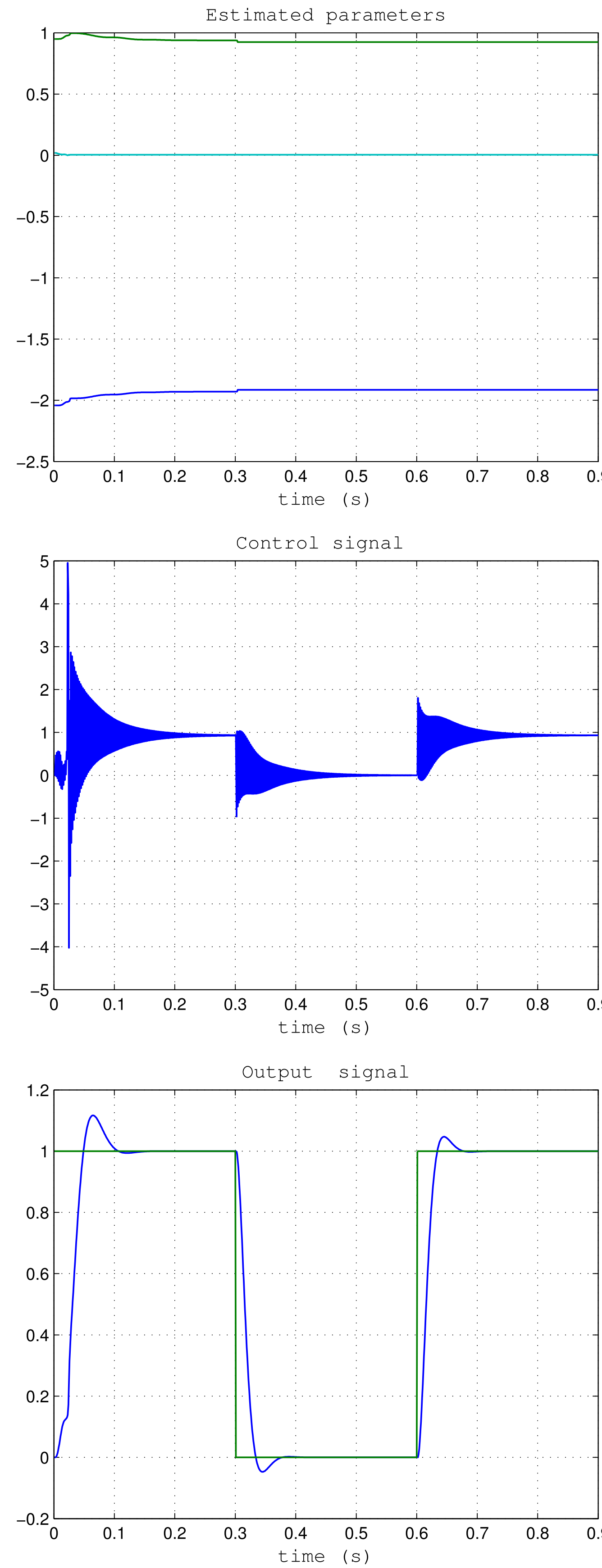

Fig. 10. Integer order adaptive pole placement control of capstan drive (Ideal case).

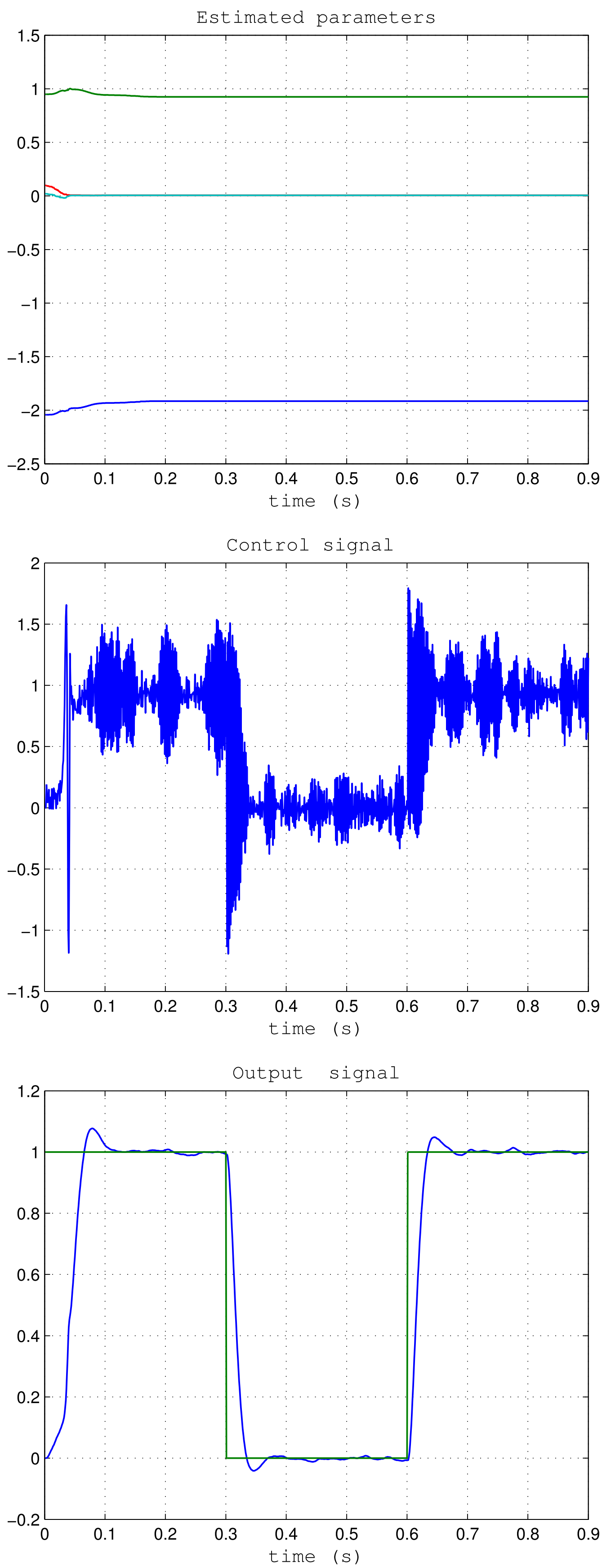

Fig. 11. Integer order adaptive pole placement control of capstan drive (with 10% magnitude input noises).

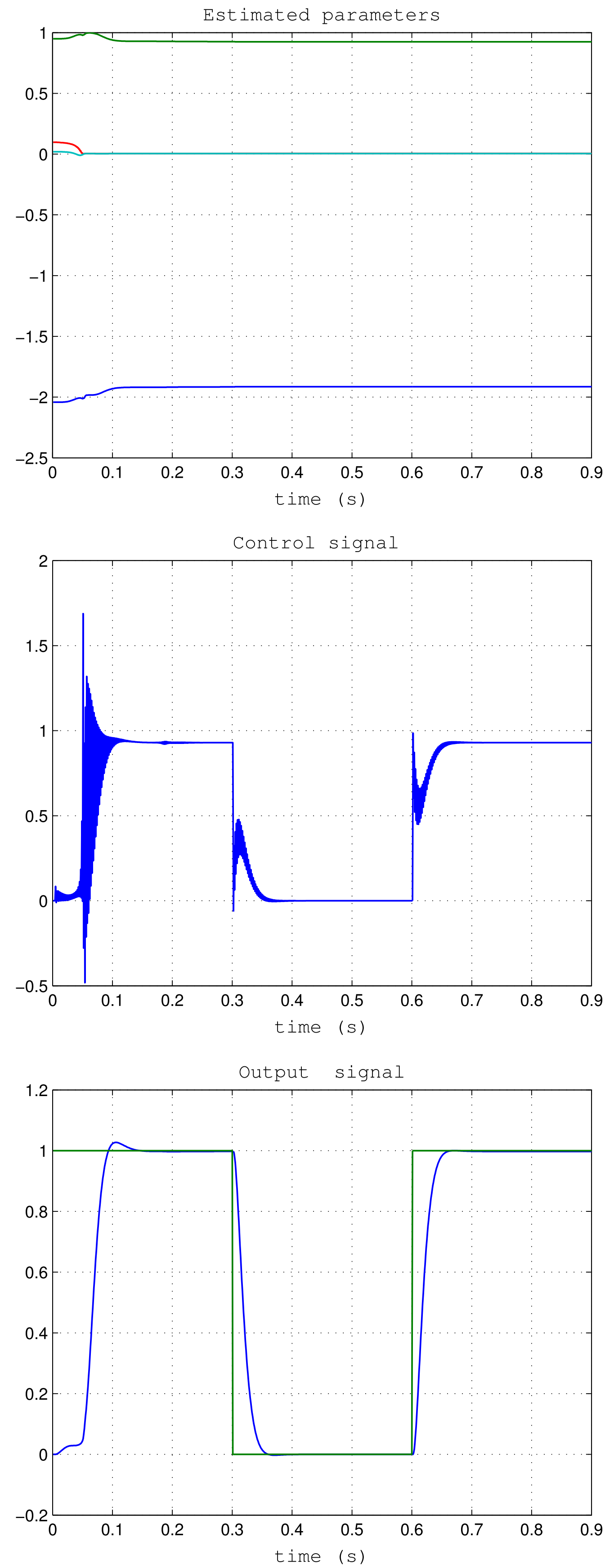

Fig. 12. Fractional order adaptive pole placement control of capstan drive for $\beta = 0.45$ (Ideal case).

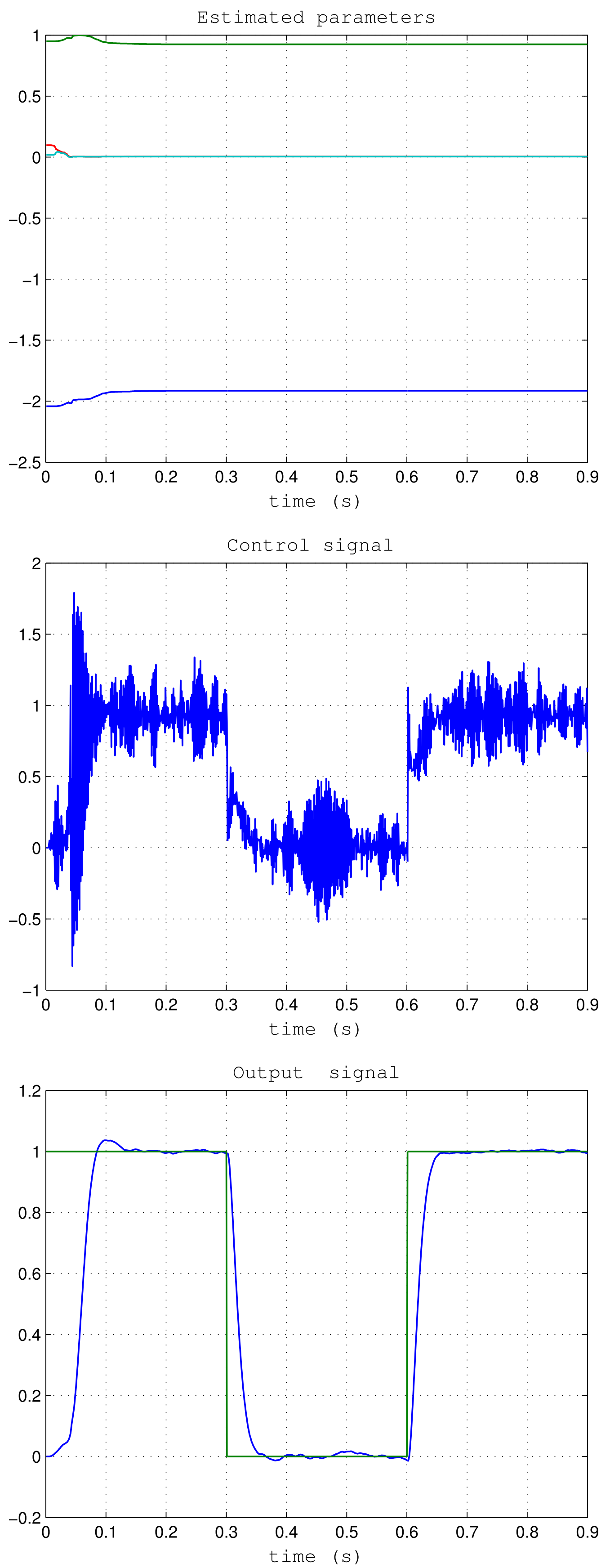

Fig. 13. Fractional order adaptive pole placement control of capstan drive $\beta = 0.45$ (with 10% magnitude input noises).

Table 3
Quadratic error criteria VS capstan drive fractional control order.

β	I_β Without perturbation	I_β With additive input perturbation
0.35	8.88	7.61
0.45	7.49	6.93
0.55	5.11	5.10
0.65	6.51	5.61
0.7	**2.81**	**2.80**
0.75	2.84	2.84
0.8	6.08	5.51
1	**4.94**	**5.79**

The use of bold points out results obtained for the integer order (1) vs. the best fractional order.

In order to quantify the disturbance rejection improvement in the fractional order control scheme, let us use the quadratic error criteria defined in Equation (38) for different values of the fractional order model reference transfer function power. The comparative results are presented in Table 3.

It is obvious that the fractional order adaptive control scheme offers generally better results regarding noises rejection and reference signal following. The optimal Index value is obtained for $\beta = 0.7$, and the system response is illustrated in Fig. 14.

One can remark that for most values of the fractional power β the quadratic error criteria show lower values in the presence of additive random input noises than in the ideal case, which is justified by the faster convergence of the estimation algorithm as the additive input random noises offer a better excitation to the system [36].

For this control objective, the fractional order pole power plays the role of a filtering parameter that offers a supplementary degree of freedom for the designer in robustness and performance adjustment tasks as illustrated by Fig. 15, which draws the error criteria evolution versus fractional poles order in presence of disturbances for both simulation examples.

This robustness property of the proposed simple fractional adaptive pole placement controller allows us to avoid more complicated 'robustified' control schemes.

5. Conclusion

In this paper, a new fractional adaptive control scheme is proposed. The control strategy combines the classical minimal degree pole placement with the process model parameters estimation in real time. The desired fractional order dynamics are imposed to the system closed loop by mean of a second order like non-integer transfer function that is approximated using the famous singularity function approximation method. The pole placement adaptive control algorithm is then applied to compute the control signals based on the on-line identified process model.

The aim of the suggested design procedure is to make the controlled plant follow the reference with improved performance behavior and good robustness against disturbance and noises. The simulation results on a DC motor angular velocity control and an air-lubricated slide/capstan-drive positioning system have confirmed the improved quality of the proposed adaptive control with fractional pole placement and on-line process model identification.

Acknowledgments

The authors would like to thank Professor Abdelfatah Charef for a number of excellent comments which improved the quality of the paper. The authors are also grateful to all the anonymous Reviewers for several good suggestions and clarifications.

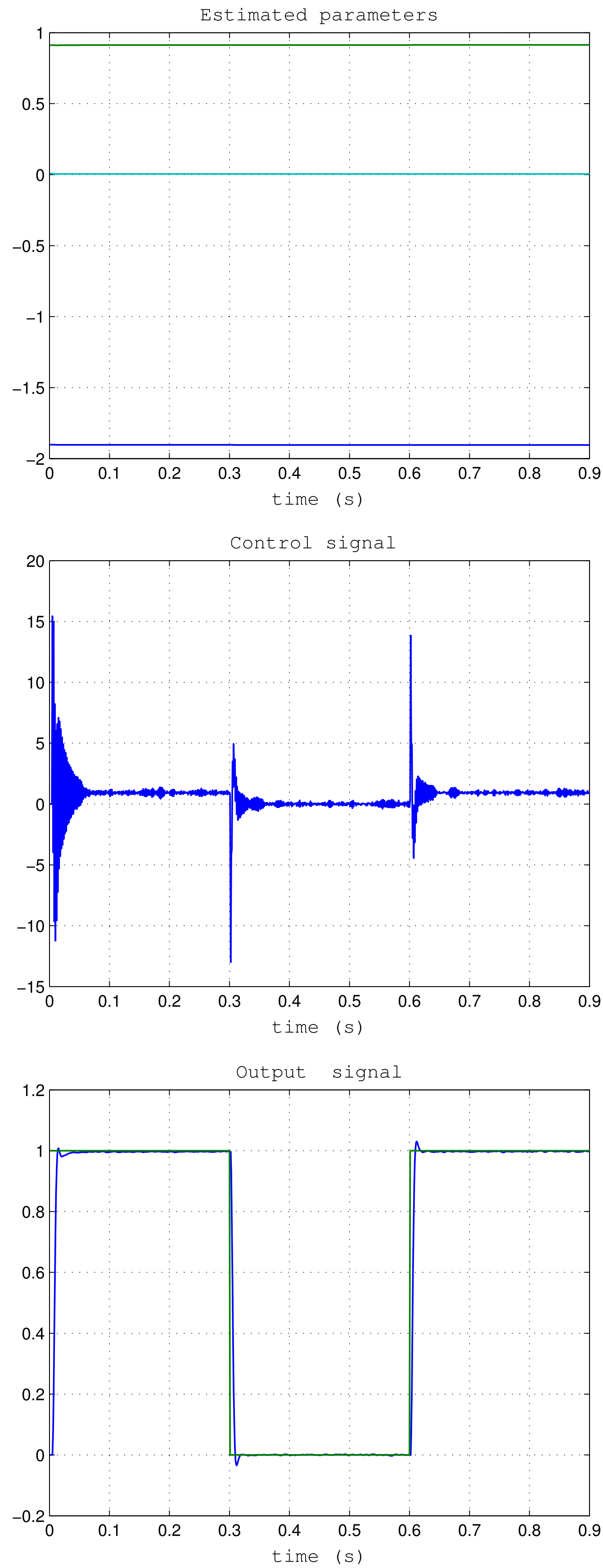

Fig. 14. Fractional order adaptive pole placement control of capstan drive $\alpha = 0.7$: Best results.

Fig. 15. Error Index versus fractional poles order in presence of noises for both simulation examples.

References

[1] S. Ladaci, A. Charef, Fractional order adaptive control systems: a survey, in: E.W. Mitchell, S.R. Murray (Eds.), Classification and Application of Fractals, Nova Science Publishers, USA, 2012, pp. 261–275.
[2] B.M. Vinagre, I. Petras, I. Podlubny, Y.-Q. Chen, Using fractional order adjustment rules and fractional order reference models in model-reference adaptive control, Nonlinear Dyn. 29 (1–4) (2002) 269–279.
[3] S. Ladaci, A. Charef, Fractional order model reference adaptive control of a robot arm, Rev. Commun. Sci. Technol. 1 (2002) 50–52 (in French).
[4] S. Ladaci, A. Charef, On fractional adaptive control, Nonlinear Dyn. 43 (4) (2006) 365–378.
[5] Y. Bensafia, S. Ladaci, Adaptive control with fractional order reference model, Int. J. Sci. Tech. Automat Control Comput. Eng. 5 (2) (2011) 1614–1623.
[6] N. Aguila-Camacho, M.A. Duarte-Mermoud, Fractional adaptive control for an automatic voltage regulator, ISA Trans. 52 (2013) 807–815.
[7] Y. Wei, Z. Sun, Y. Hu, Y. Wang, On fractional order composite model reference adaptive control, Int. J. Syst. Sci. (2015) doi:10.1080/00207721.2014.998749.
[8] M. Abedini, M.A. Nojoumian, H. Salarieh, A. Meghdari, Model reference adaptive control in fractional order systems using discrete-time approximation methods, Commun. Nonlinear Sci. Numer. Simul. 25 (2015) 27–40.
[9] H. Delavari, R. Ghaderi, N.A. Ranjbar, S.H. HosseinNia, S. Momani, Adaptive fractional PID controller for robot manipulator, Proceedings of the 4th IFAC Workshop Fractional Differentiation and its Applications, FDA'10, vol. 4, Badajoz, Spain, October 18–20, 2010.
[10] A. Neçaibia, S. Ladaci, Self-tuning fractional order $PI^{\lambda}D^{\mu}$ controller based on extremum seeking approach, Int. J. Automat. Control 8 (2) (2014) 99–121.
[11] S. Ladaci, J.J. Loiseau, A. Charef, Fractional order adaptive high-gain controllers for a class of linear systems, Commun. Nonlinear Sci. Numer. Simul. 13 (4) (2008) 707–714.
[12] A. Charef, M. Assabaa, S. Ladaci, J.J. Loiseau, Fractional order adaptive controller for stabilized systems via high-gain feedback, IET Control Theory Appl. 7 (6) (2013) 822–828.
[13] S. Ladaci, J.J. Loiseau, A. Charef, Adaptive internal model control with fractional order parameter, Int. J. Adapt. Control Signal Process. 24 (11) (2010) 944–960.
[14] M.O. Efe, ADALINE based robust control in robotics: a Riemann–Liouville fractional differintegration based learning scheme, Soft Comput. 13 (1) (2009) 23–29.
[15] S. Ladaci, A. Charef, J.J. Loiseau, Robust fractional adaptive control based on the strictly positive realness condition, Int. J. Appl. Math. Comput. Sci. 19 (1) (2009) 69–76.
[16] A. Neçaibia, S. Ladaci, A. Charef, J.J. Loiseau, Fractional order extremum seeking control, Proceedings of 22nd Mediterranean Conference on Control and Automation, MED'14, Palermo, Italy, June 16–19, 2014, pp. 459–462.
[17] J.I. Suárez, B.M. Vinagre, Y.-Q. Chen, A fractional adaptation scheme for lateral control of an AGV, Proceedings of 2nd IFAC Workshop on Fractional Differentiation and its Applications, FDA'06, Porto, Portugal, July 19–21, 2006.
[18] J. Ma, Y. Yao, D. Liu, Fractional order model reference adaptive control for a hydraulic driven flight motion simulator, Proceedings of 41st Southeastern

Symposium on System Theory University of Tennessee Space Institute Tullahoma, TN, USA, March 15–17, 2009, pp. 340–343.
[19] Y. Luo, Y.-Q. Chen, H.-S. Ahn, Fractional order adaptive compensation for cogging effect in PMSM position servo systems, Proceedings of 3rd IFAC Workshop on Fractional Differentiation and its Applications, FDA'08, Ankara, Turkey, 5–7 November, 2008.
[20] H. Malek, Y.-Q. Chen, BICO MPPT: a faster maximum power point tracker and its application for photovoltaic panels, Int. J. Photoenergy 2014 (2014) 586503.
[21] C. Yin, B. Stark, Y.-Q. Chen, S.-M. Zhong, E. Lau, Fractional-order adaptive minimum energy cognitive lighting control strategy for the hybrid lighting system, Energy Build. 87 (2015) 176–184.
[22] A. Neçaibia, S. Ladaci, A. Charef, J.J. Loiseau, Fractional order extremum seeking approach for maximum power point tracking of photovoltaic panels, Front. Energy 9 (1) (2015) 43–53.
[23] A. Charef, H.H. Sun, Y.Y. Tsao, B. Onaral, Fractal system as represented by singularity function, IEEE Trans. Automat. Control 37 (9) (1992) 1465–1470.
[24] K. Miller, B. Ross, An Introduction to the Fractional Calculus and Fractional Differential Equations, Wiley, New York, 1993.
[25] I. Podlubny, Fractional Differential Equations, Academic Press, San Diego, CA, USA, 1999.
[26] A. Oustaloup, The CRONE Control, Hermès, Paris, 1991.
[27] J.A.T. Machado, Analysis and design of fractional-order digital control systems, Syst. Anal. Model. Simul. 27 (1997) 107–122.
[28] I. Podlubny, Fractional-order systems and $PI^{\lambda}D^{\mu}$-controllers, IEEE Trans. Automat. Control 44 (1) (1999) 208–214.
[29] J.A.T. Machado, Discrete-time fractional-order controllers, Fract. Calc. Appl. Anal. 4 (2001) 47–66.
[30] A. Charef, Analogue realisation of fractional-order integrator, differentiator and fractional $PI^{\lambda}D^{\mu}$ controller, IEE Proc. Control Theory Appl. 153 (2006) 714–720.
[31] H. Sun, A. Charef, Fractal system – a time domain approach, Ann. Biomed. Eng. 18 (6) (1990) 597–621.
[32] K.J. Åström, B. Wittenmark, Adaptive Control, Addison-Wesley Publishing Company, Inc., New York, 1995.
[33] D. Xue, C. Zhao, Y.-Q. Chen, Fractional order PID control of A DC-Motor with elastic shaft: a case study, Proceedings of the 2006 American Control Conference, Minneapolis, Minnesota, USA, June 14–16, 2006.
[34] C.L. Chao, J. Neou, Model reference adaptive control of air-lubricated capstan drive for precision positioning, Precis. Eng. 24 (2000) 285–290.
[35] S. Ladaci, Y. Bensafia, Fractionalization: a new tool for robust adaptive control of noisy plants, Proceedings of 6th IFAC Workshop on Fractional Differentiation and Its Applications, FDA'13, Grenoble, France, February 4–6, 2013, pp. 379–384.
[36] I. Barkana, Gain conditions and convergence of simple adaptive control, Int. J. Adapt. Control Signal Process. 19 (2005) 13–40.